polymyositis (DM/PM). The diagnoses were made based on the clinical features, histochemical and immunohistochemical analyses of skeletal muscle biopsy specimens. Genetic diagnoses were also made in some cases. The patients with no obvious pathological changes in the skeletal muscle specimens were included as normal controls.

2.2. Immunoblot analysis of β-dystroglycan in the biopsied skeletal muscles

The skeletal muscle specimens were extracted quickly by homogenizing and boiling in a buffer containing 80 mM Tris-HCl, pH 6.8, 10% SDS, 1% β-mercaptoethanol and 115 mM sucrose, in the presence of protease inhibitors, including 0.6 mg/ml pepstatin A, 0.5 mg/ml aprotinin, 0.5 mg/ml leupeptin, 1 mM benzamidine, 1 mM PMSF, 1 mM EDTA, 1 mM EGTA and 20 mg/ml N-Biphenylsulfonyl-phenylalanine hydroxamic acid (a kind gift from Shionogi & Co. Ltd), as described previously [6,7,10]. 3–15% SDS-polyacrylamide gel electrophoresis and immunoblotting were performed as described previously [6,7,10]. The proteolysis of β-dystroglycan was detected by the monoclonal antibody 43DAG/8D5 against the C-terminus of β-dystroglycan (a kind gift from Dr L. V. B. Anderson of Newcastle General Hospital) [6,7,11]. Immunoblot development was done by enhanced chemiluminescence (Pierce) and visualized by Image Station 440 system (Eastman Kodak Company, New Haven, CT). The band intensity of β-DG_{30} and the full-size 43 kDa β-dystroglycan (β-DG_{full}) was measured using 1D image analyzing software and the ratio of β-DG_{30} against β-DG_{full} (β-DG_{30}/β-DG_{full} ratio) was calculated for each patient. The average value of the β-DG_{30}/β-DG_{full} ratio was obtained for normal control and various muscular diseases. The statistical difference among the groups was first tested using one factor ANOVA and then the difference between normal control and each disease group was evaluated by Dunnett's analysis.

3. Results

The results are summarized in Table 1 and Fig. 1. The actual immunoblots of some of the patients are shown in Fig. 2. Although there was some variation among patients, a 30 kDa band corresponding to β-DG_{30} was clearly observed in all the patients with SGCP and DMD (Table 1 and Fig. 2). Statistical analysis demonstrated significant increase of the β-DG_{30}/β-DG_{full} ratio in SGCP and DMD, compared to normal control (Table 1 and Fig. 1). On the other hand, statistical analysis did not demonstrate significant increase of the β-DG_{30}/β-DG_{full} ratio in BMD, FCMD, MM, LGMD2A, FSHD, DM and DM/PM, compared to normal control (Table 1 and Fig. 1), although mild proteolysis was detectable in some individuals (Table 1 and Fig. 2).

We performed the histochemical analysis of skeletal muscle biopsy specimens in order to see if pathological changes were correlated with the increase of proteolysis of β-dystroglycan. The severity of the pathological changes

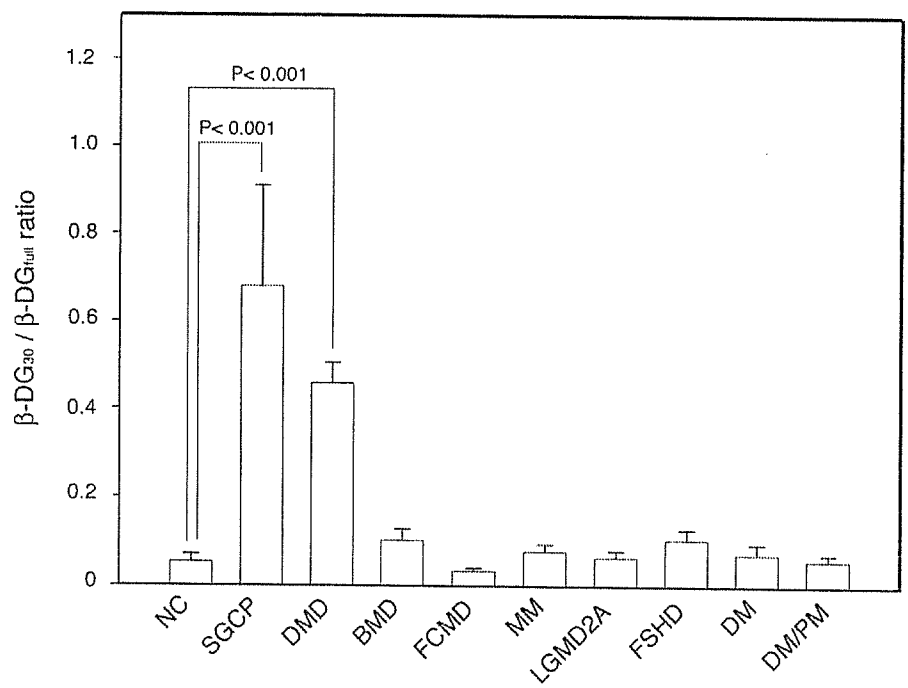

Fig. 1. The ratio of β-DG_{30} against β-DG_{full} in various muscular diseases.The average value of the β-DG_{30}/β-DG_{full} ratio was obtained for normal control and various muscular diseases. The statistical difference among the groups was first tested using one factor ANOVA and then the difference between normal control and each disease group was evaluated by Dunnett's analysis. The β-DG_{30}/β-DG_{full} ratio was significantly increased in SGCP ($P < 0.001$) and DMD ($P < 0.05$), compared to normal control. There was no significant difference between other disease groups and normal control. Error bar indicates standard error.

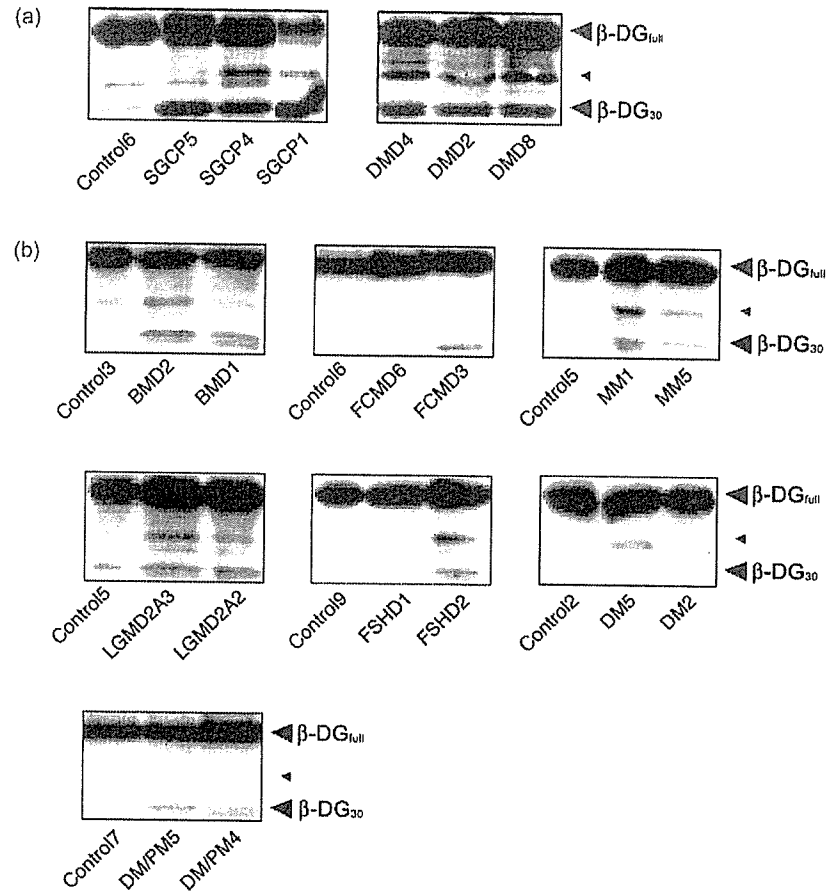

Fig. 2. Immunoblot analysis of β-dystroglycan in the skeletal muscle biopsy specimens of various muscular diseases.The skeletal muscle biopsy specimens were analyzed by immunoblotting using the monoclonal antibody 43DAG/8D5. SGCP and DMD are shown in (a) and BMD, FCMD, MM, LGMD2A, FSHD, DM and DM/PM are shown in (b). Except DMD, equal amount of proteins were loaded for each lane, using myosin heavy chain as internal standard as described previously [10]. For DMD, approximately three times volume of normal control was loaded to visualize β-dystroglycan which is severely reduced in this disease [17]. The band indicated by the small a nrrowhead corresponds to what we reported previously as the intermediate proteolytic fragment of β-DG$_{full}$ [6,7].

was variable not only among the different disease groups but also among the patients with the same disease (Fig. 3). Overall, however, necrotic muscle fibers were observed most frequently in DM/PM, and less frequently in DMD, SGCP and MM (Fig. 3). Hypercontracted muscle fibers were observed most frequently in DMD and SGCP, and less frequently in BMD, DM/PM and FCMD (Fig. 3). Necrotic and hypercontracted muscle fibers were observed infrequently in the other diseases (Fig. 3). Interstitial fibrosis and infiltration of inflammatory cells were mostprominent in FCMD and DM/PM, respectively (Fig. 3).

4. Discussion

Disruption of the tight linkage between the ECM and cell membrane provided by the dystroglycan complex is presumed to have a deleterious effect on the stability of sarcolemma and viability of muscle cells [2,3,6]. Several mechanisms are conceivable that disrupt this linkage. One is the defective glycosylation of β-dystroglycan, which has been demonstrated in several forms of severe congenital muscular dystrophies [for review, see 12–15]. In these diseases, primary defects of the genes encoding the putative glycosyltransferases disturb the glycosylation of β-dystroglycan crucial for the binding of laminin [16] and result in the disruption of the ECM-cell membrane linkage via the dystroglycan complex [12–15]. Recent evidence indicates that the interaction of a glycosyltransferase LARGE with the N-terminal domain of β-dystroglycan is necessary to initiate the posttranslational glycosylation within the mucin domain of β-dystroglycan [17]. The MMP activity that cleaves the extracellular domain of β-dystroglycan is another mechanism that can disrupt this linkage [6]. In the previous study, we showed that this MMP activity was activated in the skeletal and cardiac muscles of cardiomyopathic hamsters, the model animals of SGCP, resulting in the disruption of the dystroglycan complex [7]. Importantly, we showed that this phenomenon was not an in vitro artifact but rather occurred in vivo [7].

In this study, we investigated the proteolysis of β-dystroglycan in the biopsied skeletal muscles of various

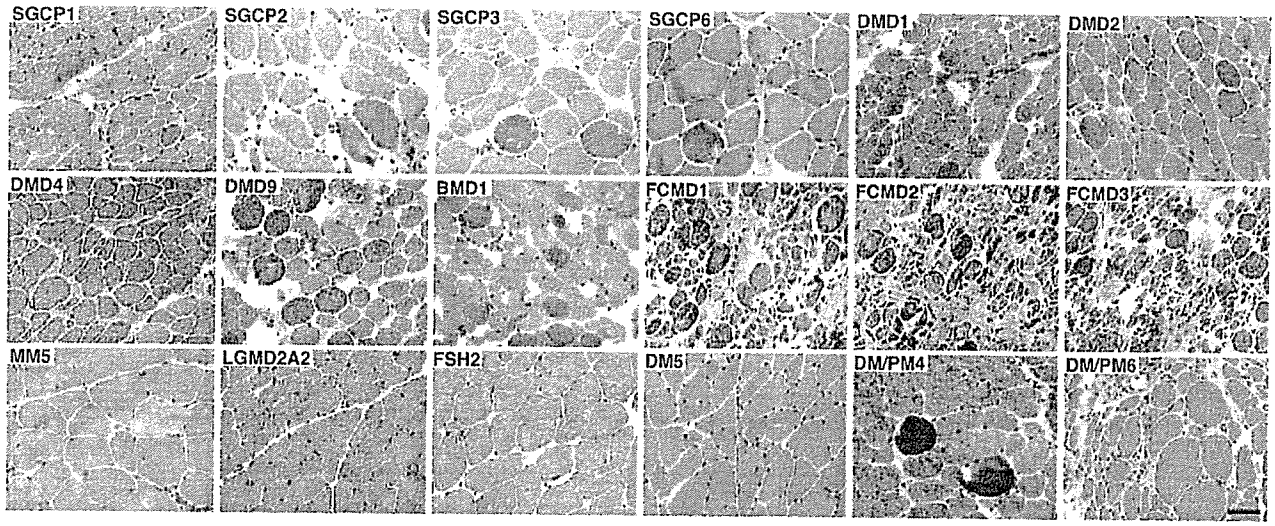

Fig. 3. Histochemical analysis of the skeletal muscle biopsy specimens.The skeletal muscle biopsy specimens were analyzed by staining with hematoxylin and eosin. The severity of the pathological changes was variable not only among the different disease groups but also among the patients with the same disease. Overall, necrotic muscle fibers were observed most frequently in DM/PM, and less frequently in DMD, SGCP and MM. Hypercontracted muscle fibers were observed most frequently in DMD and SGCP, and less frequently in BMD, DM/PM and FCMD. Necrotic and hypercontracted muscle fibers were infrequently observed in the other diseases. Interstitial fibrosis and infiltration of inflammatory cells were most prominent in FCMD and DM/PM, respectively. Bar, 50 μm.

human muscular diseases. We found that the proteolysis of β-dystroglycan was increased significantly in SGCP and DMD. The present results confirm the previous observation by Anderson and Davison, who referred to a similar phenomenon in the biopsied skeletal muscles of SGCP patients [11]. However, they attributed this to the artificial degradation and did not present the results in details [11]. Together with the aforementioned results in cardiomyopathic hamsters [7], we propose that the proteolysis of β-dystroglycan in SGCP is not an in vitro artifact but rather occurs in vivo. On the other hand, this study is the first to report the increased proteolysis of β-dystroglycan in DMD.

At present, the mechanism by which the proteolysis of β-dystroglycan is increased in SGCP and DMD remains obscure. In this respect, it should be noted that hypercontracted muscle fibers were observed frequently in the patients with SGCP and DMD, raising a possibility that the proteolysis of β-dystroglycan may reflect the active degeneration process of muscle fibers. However, the proteolysis of β-dystroglycan was not severe in the patients with BMD and DM/PM who had numerous hypercontracted muscle fibers (for instance, BMD1 and DM/PM4 of Fig. 3). These results suggest that other or additional mechanisms may be present that contribute to the proteolysis of β-dystroglycan. For instance, it is possible that the deficiency of the sarcoglycan complex may render β-dystroglycan susceptible to proteolysis, because it is well established that the sarcoglycan complex is specifically and drastically reduced in these two diseases [18]. In any case, the resulting proteolysis of β-dystroglycan will disrupt the link between the ECM and cell membrane via the dystroglycan complex and render muscle fibers susceptible to further degeneration.

The proteolysis of β-dystroglycan was not significantly increased in BMD, FCMD, MM, LGMD2A, FSHD, DM and DM/PM, although mild proteolysis was detectable in some individuals. When we initiated this study, we were particularly interested if the proteolysis of β-dystroglycan by MMP was activated in FCMD. In FCMD skeletal muscle, the glycosylation of β-dystroglycan crucial for the binding of laminin is disturbed, resulting in the disruption of the ECM-cell membrane linkage via the dystroglycan complex [19]. We wondered if this might render β-dystroglycan susceptible to proteolysis but have found that this is not the case in this study. We also wondered if the proteolysis of β-dystroglycan was increased in DM/PM, because various MMPs are reported activated in inflammatory myopathies [20–22]. However, this did not turn out to be the case in this study. Our results suggest that the MMP that cleaves the extracellular domain of β-dystroglycan may be distinct from those reported activated in inflammatory myopathies.

Acknowledgements

We thank Miki Yamanaka and Yuka Sasayama for their expert technical assistance. This work was supported by [1] Research Grants 14B-4 and 16B-1 for Nervous and Mental Disorders (Ministry of Health, Labor and Welfare), [2] Research on Psychiatric and Neurological Diseases and Mental Health (Ministry of Health, Labor and Welfare), and [3] Research Grant 16390256 and 'High-Tech Research Center' Project for Private Universities: matching fund subsidy from MEXT (Ministry of Education, Culture, Sports, Science and Technology), 2004–2008.

References

[1] Ibraghimov-Beskrovnaya O, Ervasti JM, Leveille CJ, Slaughter CA, Sernett SW, Campbell KP. Primary structure of dystrophin-associated glycoproteins linking dystrophin to the extracellular matrix. Nature 1992;355:696–702.

[2] Henry MD, Campbell KP. Dystroglycan: an extracellular matrix receptor linked to the cytoskeleton. Curr Opin Cell Biol 1996;8:625–31.

[3] Winder SJ. The complexities of dystroglycan. Trends Biochem Sci 2001;26:118–24.

[4] Stasio ED, Sciandra F, Maras B, et al. Structural and functional analysis of the N-terminal extracellular region of β-dystroglycan. Biochem Biophys Res Comm 1999;206:274–8.

[5] Ishikawa-Sakurai M, Yoshida M, Imamura M, Davies KE, Ozawa E. ZZ domain is essentially required for the physiological binding of dystrophin and utrophin to β-dystroglycan. Hum Molec Genet 2004; 13:693–702.

[6] Yamada H, Saito F, Fukuta-Ohi H, et al. Processing of β-dystroglycan by matrix metalloproteinase disrupts the link between the extracellular matrix and cell membrane via the dystroglycan complex. Hum Molec Genet 2001;10:1563–9.

[7] Matsumura K, Arai K, Zhong D, et al. Disruption of dystroglycan axis by β-dystroglycan processing in cardiomyopathic hamster muscle. Neuromusc Disord 2003;13:796–803.

[8] Nigro V, Okazaki Y, Belsito A, et al. Identification of the Syrian hamster cardiomyopathy gene. Hum Molec Genet 1997; 6:601–7.

[9] Sakamoto A, Ono K, Abe M, et al. Both hypertrophic and dilated cardiomyopathies are caused by mutation of the same gene, δ-sarcoglycan, in hamster: an animal model of disrupted dystrophin-associated glycoprotein complex. Proc Natl Acad Sci USA 1997;94: 13873–8.

[10] Matsumura K, Tome FMS, Collin H, et al. Deficiency of the 50K dystrophin-associated glycoprotein in severe childhood autosomal recessive muscular dystrophy. Nature 1992;359:320–2.

[11] Anderson LVB, Davison K. Multiplex western blotting system for the analysis of muscular dystrophy patients. Am J Pathol 1999;154: 1017–22.

[12] Martin-Rendon E, Blake DJ. Protein glycosylation in disease: new insights into the congenital muscular dystrophies. Trends Pharmacol Sci 2003;24:178–83.

[13] Grewal PK, Hewitt JE. Glycosylation defects: a new mechanism for muscular dystrophy? Hum Molec Genet 2003;12: 259–64.

[14] Endo T, Toda T. Glycosylation in congenital muscular dystrophies. Biol Pharm Bull 2003;26:1641–7.

[15] Muntoni F, Brockington M, Torelli S, Brown SC. Defective glycosylation in congenital muscular dystrophies. Curr Opin Neurol 2004;17:205–9.

[16] Chiba A, Matsumura K, Yamada H, et al. Structures of sialylated O-linked oligosaccharides of bovine peripheral nerve α-dystroglycan: the role of a novel mannosyl type oligosaccharide in the binding with laminin. J Biol Chem 1997;272:2156–62.

[17] Kanagawa M, Saito F, Kunz S, et al. Molecular recognition by LARGE is essential for expression of functional dystroglycan. Cell 2004;117:953–64.

[18] Ohlendieck K, Matsumura K, Ionasescu VV, et al. Duchenne muscular dystrophy: deficiency of dystrophin-associated proteins in the sarcolemma. Neurology 1993;43:795–800.

[19] Michele DE, Barresi R, Kanagawa M, et al. Post-translational disruption of dystroglycan–ligand interactions in congenital muscular dystrophies. Nature 2002;418:417–22.

[20] Choi YC, Dalakas MC. Expression of matrix metalloproteinases in the muscle of patients with inflammatory myopathies. Neurology 2000; 54:65–71.

[21] Kieseier BC, Schneider C, Clements JM, et al. Expression of specific matrix metalloproteinases in inflammatory myopathies. Brain 2001; 124:341–51.

[22] Schoser BG, Blottner D, Stuerenburg HJ. Matrix metalloproteinases in inflammatory myopathies: enhanced immunoreactivity near atrophic myofibers. Acta Neurol Scand 2002;105:309–13.

PERGAMON

Neuromuscular Disorders 15 (2005) 342–348

www.elsevier.com/locate/nmd

Congenital muscular dystrophy with glycosylation defects of α-dystroglycan in Japan

Hiroshi Matsumoto[a,e], Yukiko K. Hayashi[a,*], Dae-Son Kim[a], Megumu Ogawa[a], Terumi Murakami[a], Satoru Noguchi[a], Ikuya Nonaka[a], Tomoyuki Nakazawa[b], Takiko Matsuo[c], Satoshi Futagami[d], Kevin P. Campbell[f], Ichizo Nishino[a]

[a]*Department of Neuromuscular Research, National Institute of Neuroscience, National Center of Neurology and Psychiatry (NCNP), 4-1-1 Ogawahigashi, Kodaira, Tokyo 187-8502, Japan*
[b]*Department of Pediatrics, Juntendo University, Tokyo, Japan*
[c]*The Tokyo Children's Rehabilitation Hospital, Tokyo, Japan*
[d]*Department of Pediatric Rehabilitation, NTT Izu Hospital, Shizuoka, Japan*
[e]*Department of Pediatrics, National Defense Medical College, Saitama, Japan*
[f]*Department of Physiology and Biophysics and Department of Neurology, Howard Hughes Medical Institute, University of Iowa, Iowa city, IA, USA*

Received 8 November 2004; received in revised form 19 January 2005; accepted 27 January 2005

Abstract

Glycosylation defects of α-dystroglycan (α-DG) cause various muscular dystrophies. We performed clinical, pathological and genetic analyses of 62 Japanese patients with congenital muscular dystrophy, whose skeletal muscle showed deficiency of glycosylated form of α-DG. We found, the first Japanese patient with congenital muscular dystrophy 1C with a novel compound heterozygous mutation in the fukutin-related protein gene. Fukuyama-type congenital muscular dystrophy was genetically confirmed in 54 of 62 patients. Two patients with muscle–eye–brain disease and one Walker-Warburg syndrome were also genetically confirmed. Four patients had no mutation in any known genes associated with glycosylation of α-DG. Interestingly, the molecular mass of α-DG in the skeletal muscle was similar and was reduced to ~90 kDa among these patients, even though the causative gene and the clinico-pathological severity were different. This result suggests that other factors can modify clinical features of the patients with glycosylation defects of α-DG.

Keywords: α-dystroglycan (α-DG); Fukuyama-type congenital muscular dystrophy (FCMD); Congenital muscular dystrophy 1C (MDC1C); Muscle-eye-brain disease (MEB); Walker-Warburg syndrome (WWS); Glycosylation; Fukutin; FKRP; POMGnT1; POMT1; LARGE

1. Introduction

Recent advances demonstrated that glycosylation defects of cell surface membrane protein, α-dystroglycan (α-DG) cause a group of muscular dystrophy, including Fukuyama-type congenital muscular dystrophy (FCMD), muscle–eye–brain disease (MEB), Walker-Warburg syndrome (WWS), congenital muscular dystrophy 1C (MDC1C) and its allelic limb-girdle muscular dystrophy (LGMD) 2I, and congenital muscular dystrophy 1D (MDC1D) [1–8]. Some of these forms are associated with neuronal migration disorder in brain and ocular abnormalities, and others with normal brain and eyes. Characteristically, they all show abnormally glycosylated α-DG with preserved core structure in the muscle sarcolemma [9]. From this result, the responsible gene products of these diseases are thought to have a role in the glycosylation process of α-DG. In fact, mutations in the glycosyltransferase genes of protein *O*-mannose β 1,2-*N*-acetylglucosaminyltransferase 1 (*POMGnT1*) and protein *O*-mannosyltransferase 1 (*POMT1*) have been identified in patients with MEB and WWS, respectively [3,4]. In addition, other responsible gene products of fukutin, fukutin-related protein (FKRP), and LARGE are also predicted to have structural similarity to glycosyltransferases [10].

In Japan, FCMD is the most common form of congenital muscular dystrophy (CMD) [11], whereas merosin-deficient

* Corresponding author. Tel.: +81 42 341 2712; fax: +81 42 346 1742.
E-mail address: hayasi_y@ncnp.go.jp (Y.K. Hayashi).

0960-8966/$ - see front matter © 2005 Elsevier B.V. All rights reserved.
doi:10.1016/j.nmd.2005.01.009

CMD (MDC1A), which is common in European countries, MEB, and WWS were rarely seen [12,13]. Patients with MDC1C and MDC1D have not been identified yet in Japan. To know more about the CMD patients with glycosylation defects of α-DG in Japan, we performed detailed genetic and clinico-pathological analyses on 62 patients.

2. Materials and Methods

2.1. Clinical materials

All clinical materials were obtained for diagnostic purposes with informed consent. We analyzed a total of 62 patients whose limb-muscle specimens showed altered glycosylation of α-DG. The clinical diagnoses of the 62 patients are shown in Table 1. The muscle samples were flash-frozen in isopentane chilled with liquid nitrogen.

2.2. Immunohistochemistry, immunoblotting, and laminin overlay assay

The following antibodies were used for immunohistochemical and immunoblotting analyses: monoclonal anti-α-DG (VIA4-1, Upstate Biotechnology), polyclonal goat anti-α-DG (GT20ADG) [9], monoclonal anti-laminin α2 chain (5H2, Chemicon), polyclonal anti-laminin-1 (Sigma), and monoclonal anti-β-DG (43DAG1/8D5, Novocastra Laboratories). The detailed techniques of the immunohistochemistry, immunoblotting and laminin overlay assay have been described previously [1,9].

2.3. Genetic analyses of fukutin, FKRP, POMGnT1, POMT1, and LARGE

DNA was isolated from skeletal muscle or peripheral lymphocytes using a standard technique.

To detect the 3-kb retroransposal insertion in *fukutin*, the genomic PCR was performed using two primer sets; one is designed to amplify a 375 bp product containing a part of retrotransposal insertion and the other is designed to amplify a normal 157 bp fragment (the primers were designed by Dr Toda, Osaka University). All exons and their flanking intronic regions of *fukutin* [14] were directly sequenced in patients without homozygous retrotransposal insertion using an ABI PRISM 3100 automated sequencer (PE Applied Biosystems).

Table 1
Clinical and genetic diagnosis of 62 patients

Genetic diagnosis		Clinical diagnosis	
FCMD	54	FCMD	53
		MEB	1
MEB	2	FCMD	1
		CMD	1
WWS	1	WWS	1
MDC1C	1	FCMD	1
Unknown	4	MEB	1
		WWS	3

Mutation analysis of *FKRP* was performed using the primers reported elsewhere [15].

Mutation analysis of *POMGnT1*, *POMT1*, and *LARGE* was performed by directly sequencing all exons and their flanking introns. The information on primer sequence and PCR conditions is available upon request. To detect the mutation in exon 11 of *POMGnT1* in patient 2, primers F (5′-CATTCACCTCTGTGGGTAAGC) and R (5′-AGGCC TTCACATTTCACAGC) were used.

2.4. Single-strand conformation polymorphism (SSCP) analysis of FKRP

To exclude the possibility of polymorphism, we performed SSCP analysis for the missense mutation identified in *FKRP* in patient 1, using Gene Gel Excel (Pharmacia Biotech). The amplified genomic DNA fragments using a set of primers (4-2F and 4-2R [15]) including the site of the missense mutation was electrophoresed for 600 mA at 10 °C in a Gene Phor Electrophoresis Unit (Pharmacia Biotech). One hundred chromosomes from healthy individuals were analyzed as control.

3. Results

We found the first patient with MDC1C (patient 1) in the oriental countries. *Fukutin* mutations were found in 87% of the patients examined, and two MEB (patients 2 and 3) and one WWS (patient 4) were genetically confirmed. Four patients had no mutation in the known genes associated with glycosylation defects of α-DG (Table 1).

3.1. Clinical features of the patients

Patient 1 (MDC1C) was a Japanese girl and first admitted to a hospital at 12-months old. She was the first child of nonconsanguineous healthy Japanese parents. From at birth, left eye strabismus was seen, and the floppiness and delayed motor milestones became apparent in growing. She was able to sit at 7 months, but unable to crawl or stand up at 12 months of age. She spoke some meaningful words, and no mental retardation was observed. Serum creatine kinase (CK) level was 6429 IU/l. Muscle biopsy was performed at 12 months of age and showed dystrophic changes with marked variation in fiber size, active necrotic and regenerating process, and dense interstitial fibrosis (Fig. 1A). She was diagnosed to have FCMD. At 6-years-old, generalized muscular atrophy was marked, but she could move by herself using her wheelchair. Facial and calf muscles were mildly hypertrophic and high-arched palate was seen. Tongue hypertrophy was not apparent. Cardiac dysfunction was not detected from the chest radiograph or electrocardiogram. Joint contractures

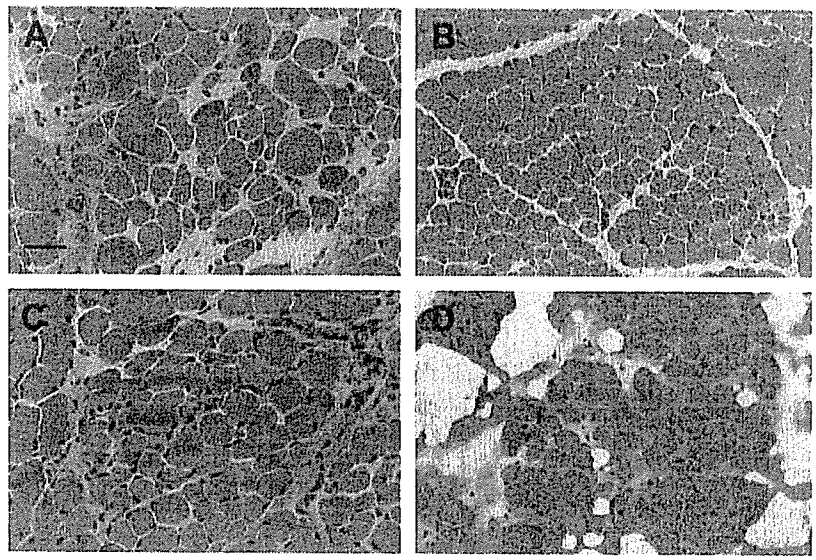

Fig. 1. Hematoxylin and eosin staining of skeletal muscles. Patient 1 (MDC1C; A), patient 3 (MEB; C), and patient 4 (WWS; D) show severe dystrophic changes with marked variation in fiber size, necrotic and regenerating fibers, and dense fibrosis in endomysium, whereas the pathological changes in patient 2 (MEB; B) is very mild, showing only mild caliber changes of muscle fibers. Bar=50 μm.

were seen in elbows, knees, and ankles. Brain magnetic resonance image (MRI) at age 5 years showed some cerebellar cysts and disorganized formation of cerebellar folia, but no structural abnormality was found in the cerebrum and the brain stem (Fig. 2A and B). Her intelligence was normal at age of 6.

Patient 2 (MEB-1) was a child of nonconsanguineous Japanese parents, and he had healthy sister and brother. He was delivered after uneventful pregnancy, and he was noted to be floppy at 4 months. At 6 months he was not able to control his head, and serum CK level was elevated to 6900 IU/l. Computed tomography of the brain showed

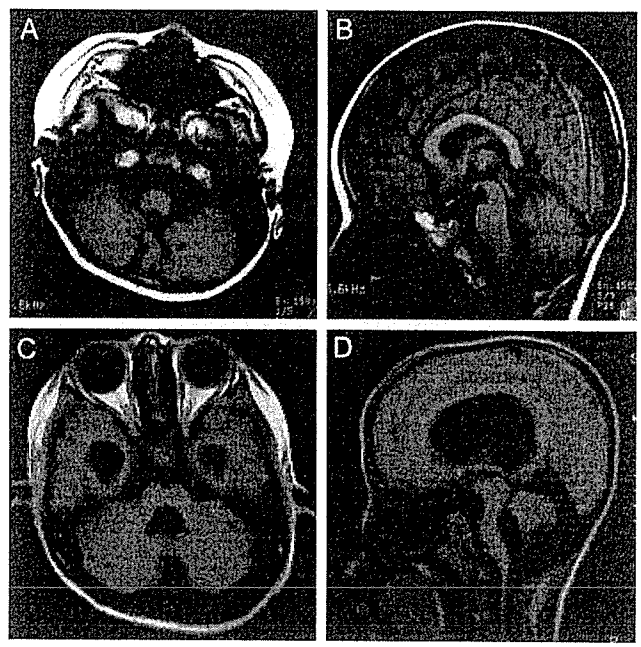

Fig. 2. Brain MRI of patient 1 (A and B) and patient 2 (C and D). T1 weighed images of patient 1 show multiple cerebellar cysts and dysmorphic cortical structures in bilateral cerebellar hemisphere (A). No abnormal findings are seen in cerebrum and brain stem (B). T1 weighed images of patient 2 show multiple cerebellar cysts (C), atrophic brain stem and markedly dilated lateral and third ventricles (D). Typical type II lissencephaly was seen in cerebrum (data not shown).

Table 2
Clinical summary of the four patients with MDC1C, MEB, and WWS

Patient no.	1 (MDC1C)	2 (MEB-1)	3 (MEB-2)[a]	4 (WWS)[b]
Age at biopsy	1 y/o	6 mo/o	1 y/o	3 y/o
Sex	F	M	F	M
Gene mutation	*FKRP*	*POMGnT1*	*POMGnT1*	*POMT1*
	266C>G,	1106insT	900G>A, 1077insG	1260_1262del CCT
	1169–1170delGC			
Mental retardation	–, DQ 110	+	+	+
Speech	Sentences	No words	No words	No words
Hydrocephalus	–	–	–	+
Type II lissencephaly	–	+	+	+
Cerebellar cysts	+	+	+	+
Brain stem hypoplasia	–	+	+	+
Eye symptoms	Strabismus	Cataract, retinal dysplasia	Myopia, retinal dysplasia	Corneal clouding
Maximum motor function	Sitting, move on buttocks	Sitting, roll over	Bed ridden	Bed ridden
CK (IU/l)	6429	6900	8019	600–31,000
Muscle pathology				
Necrosis	Occasional	Few	Occasional	Occasional
Fibrosis	Marked	Very mild	Marked	Marked

[a] Previously reported as SI [12].
[b] Previously reported [13].

dilated lateral ventricles and diffuse periventricular lucency of white matter. Brain MRI at age 10 years showed markedly dilated ventricles, type II lissencephaly, cerebellar cysts, and flat brain stem (Fig. 2C and D). Examination of eyes showed bilateral retinal degeneration. His eye problems had been progressive, and at age 10 years he received operation for bilateral cataracts. Bilateral optic nerve atrophy and detachment of retina of right eye were also found. A muscle biopsy taken at 6 months of age showed only mild dystrophic changes with a few necrotic and regenerating fibers. No marked fibrous tissue involvement was seen (Fig. 1B). He was suggested to have CMD. He was able to turn over at 22 months, but further motor development was not obtained. At age 11, he was wheel chair bound, and could move by rolling over on the floor. Contractures were seen in bilateral knee and ankle joints. In comparison with his motor function, mental retardation was severe. He could not speak any meaningful words, and could only express his pleasure or sad feelings by facial expression in response to his parents' voice.

The clinical and genetic description of patient 3 (MEB-2) was previously reported (patient SI [12]), and they are summarized in Table 2.

We recently reported the clinical features and the result of genetic analysis of Patient 4 (WWS) [13], and they are summarized in Table 2.

3.2. Patients with unknown cause

No mutation was identified in four of 62 patients who were clinically diagnosed to have MEB or WWS (Table 1). All four patients showed severe mental retardation, hypotonia from early infancy, and eye involvements. Brain MRI displayed type II lissencephaly, enlarged lateral ventricles, and hypoplastic brainstem and cerebellum. In the skeletal muscles, three patients who were clinically diagnosed as WWS showed severe dystrophic changes with marked fibrous tissue involvement. However, one patient who was clinically diagnosed as MEB showed only mild myopathic changes in his muscle.

3.3. Genetic analyses for fukutin, FKRP, POMGnT1, POMT1, and LARGE

Among 62 patients served for genetic analyses, 54 patients (87%) had 3-kb retrotransposal insertion homozygously or heterozygously (Table 3). Twelve patients had this insertion heterozygously, and we performed sequence analysis of all exons and their flanking region of *fukutin*. We identified point mutations in *fukutin* in seven patients, including one novel mutation (Table 3), but no mutation was found in the remaining five patients with 3-kb insertion in one allele.

We performed mutation screening in *FKRP*, *POMGnT1*, *POMT1*, and *LARGE* on eight patients who had no retrotransposal insertion in *fukutin*. We found a patient (patient 1) with a novel compound heterozygous mutation in *FKRP* (266C>G transversion which generate P89R, and 1169_1170 del GC which causes premature termination)

Table 3
Results of mutation analysis of *fukutin*

3-kb insertion	*Fukutin* mutation (amino acid change)	No. of patients
Homozygote	42	
Heterozygote	12	
	250C>T (R47X)	3
	626A>G (H172R)	1
	859T>G (C250G)	1
	1025G>A (W305X)[a]	1
	1169T>A (L353X)	1

[a] A novel mutation.

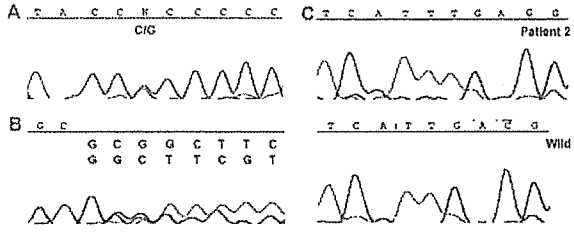

Fig. 3. Electropherograms of the sequence analysis of *FKRP* and *POMGnT1*. A novel compound heterozygous mutation in *FKRP* was identified in patient 1 with heterozygous 266C>G (A) and 1169_1170 del GC (B). Patient 2 shows homozygous 1106 ins T in *POMGnT1* (C, Patient 2).

(Fig. 3A and B). The SSCP analysis of *FKRP* showed that only this patient but not 50 healthy individuals had a mobility shift (data not shown). Two patients had mutations in *POMGnT1*. A homozygous 1106 ins T in exon 11, which generates D338fs (Fig. 3C) was seen in patient 2. Mutations of *POMGnT1* in patient 3 and *POMT1* in patient 4 were reported previously [12,13]. The remaining four patients had no mutation in the all genes examined including *LARGE*.

3.4. Immunostaining and immunoblotting analyses

In all muscles from FCMD patients, marked reduced membrane staining was seen using α-DG (VIA4-1) antibody, which recognize glycosylated form of α-DG, while β-DG immunoreaction was well preserved as previously described [1]. Immunostaining with anti-GT20ADG antibody that recognize the core region of α-DG showed positive membrane staining [9]. All eight CMD patients other than FCMD showed similar immunoreactions to those of FCMD muscles, including patient 1 with FKRP mutations (Fig. 4). Immunoreaction of laminin α2 chain in patient 1 show very mild reduction (Fig.4C). Reduced staining of laminin α2 chain was marked in FCMD and WWS patients [13], however, in the two MEB patients, nearly normal immunoreaction was seen (Fig. 4C) [12]. On immunoblotting analysis, barely detectable level of glycosylated form of α-DG was seen using VIA4-1 antibody in all the patients (Fig. 5A), whereas the GT20ADG antibody recognized more migrating bands in ~90 kDa in all patients we examined independent on the causative gene (Fig. 5B). Laminin overlay assay revealed no detectable binding

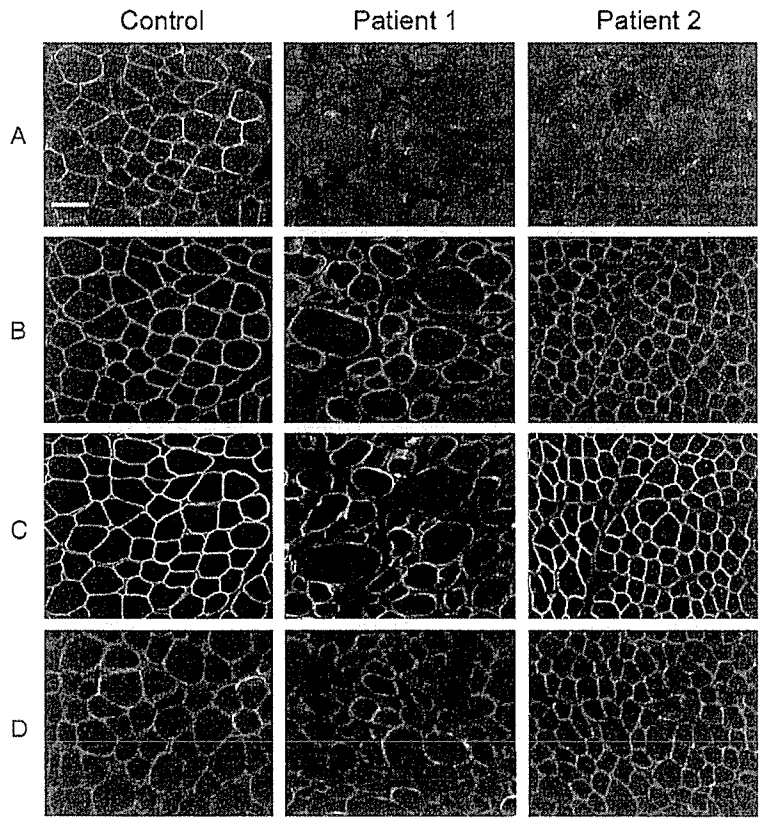

Fig. 4. Immunohistochemical analysis. Skeletal muscles from control, patient 1 (MDC1C), and patient 2 (MEB) are immunostained with antibodies against α-DG (VIA4-1; A), β-DG (B), laminin α2 chain (C), and core antibody against α-DG (GT20ADG; D). Immunoreaction for VIA4-1 is markedly reduced in patient 1 and patient 2, while β-DG is normally expressed in the sarcolemma. α-DG core protein is preserved by GT20ADG in both patients. Bar = 50 μm.

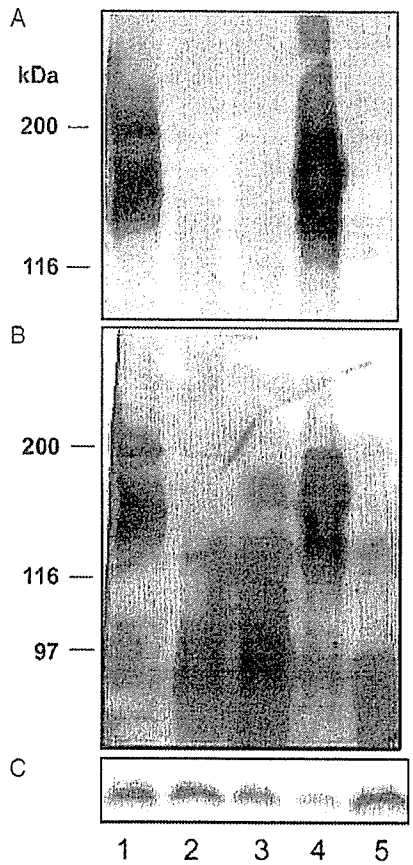

Fig. 5. Immunoblotting analysis. Skeletal muscle homogenates from control (lane 1), patient 1 (MDC1C; lane 2), FCMD (lane 3), control (lane 4), and patient 2 (MEB; lane 5) were blotted with VIA4-1 (A), GT20ADG (B), and β-DG (C) antibodies. FCMD, patient 1, and patient 2 showed barely detectable glycosylated form of α-DG by VIA4-1, whereas decreased sized bands (~90 kDa) were detected by GT20ADG.

product in the muscles with glycosylation defects of α-DG (data not shown).

4. Discussion

In this study, 86% of the patients with glycosylation defects of α-DG were genetically confirmed as FCMD, reflecting the most common form of CMD in Japan. The FCMD patients show severe muscular dystrophy with central nervous system involvements, but relative broad spectrum of clinical symptoms is known. A small number of FCMD patients can walk at some point and speak meaningful sentences, while some patients show severely affected brain and eye malformations mimicking to Walker-Warburg phenotypes [11,14]. One FCMD patient in our series with a compound heterozygous mutation (a 3-kb insertion and a Arg47stop) showed severe muscular dystrophy, hydrocephalus and retinal degeneration, and clinically diagnosed as MEB/WWS. Despite of the different clinical severity, the positive muscle fibers of glycosylated form of α-DG (VIA4-1) was very few in all FCMD patients. The molecular mass of α-DG detected by the antibody for core region (GT20ADG) were also equally reduced to ~90 kDa in all FCMD patients examined (data not shown). These results imply additional factor(s) to determine the clinical severity of FCMD.

Here, we report the first patient with MDC1C in the oriental countries. Patients with *FKRP* mutations are known to show wide variety of clinical spectrums from LGMD2I, MDC1C to severe MEB/WWS phenotypes. Recently genotype–phenotype correlations in *FKRP* mutations were reported [15]. Patients with MDC1C phenotype have a compound heterozygous mutation between a null and a missense mutation or carried two missense mutations, while common Leu276Ileu mutation was constitutionally seen in LGMD2I. Our patient had novel mutations in a combination of frameshift and missense mutations. Clinically, the patient showed severe muscle weakness from early infancy, marked elevation of serum CK level, calf hypertrophy, and normal intelligence; and those are consistent with MDC1C. Further, the structural abnormality in the cerebellum was seen on brain MRI including disorganized folia and multiple cysts, those are commonly observed in FCMD/MEB. Unlike the other forms of CMD with glycosylation defects of α-DG, central nervous system involvements are rare in the patients with *FKRP* mutations [4,5]. Only a few patients with mental retardation and cerebellar cysts were reported from Turkey and Tunisia [16,17]. More recently, two patients with MEB and WWS phenotypes caused by *FKRP* mutations were reported [18]. Although the brain involvement in MDC1C is quite rare, these reports suggest the possibility that FKRP may play some roles in normal development of the brain, especially in the cerebellum.

Skeletal muscles from patients with *FKRP* mutations show variable levels of reduction of α-DG, from nearly normal in LGMD2I to almost absent in MDC1C by using anti-α-DG (VIA4-1) antibody [15]. Our MDC1C patient displayed almost absent glycosylated form of α-DG recognized by VIA4-1, which is similar to the other severe forms of CMD with glycosylation defects of α-DG. Further, we found the preserved core peptide of α-DG in the skeletal muscle. Surprisingly, molecular mass of α-DG recognized by the core antibody was quite similar to the other related diseases including FCMD, MEB, and WWS, although brain involvement was limited. From this result, the functions of FKRP on the glycosylation process of α-DG seems to be similar in the skeletal muscle to the other related gene products for glycosylation defects of α-DG.

The broader clinical spectrum of MEB was reported recently, though MEB pedigree in Finland shows uniform clinical features [12,19]. Two genetically confirmed MEB patients identified in this study (patients 2 and 3) showed similar brain and eye involvements, but interestingly, histological findings of skeletal muscles were quite different. Patient 2 showed only mild dystrophic changes,

while patient 3 showed active necrotic and regenerating process with severe endomysial fibrosis. No difference was seen in the expression patterns and the molecular mass of α-DG detected by the core antibody. Both patients showed nearly normal expression of laminin α2 chain around muscle fibers. The homozygous insertion mutation identified in patient 2 was located in the catalytic domain, while the mutations in patient 3 was a missense mutation in the stem domain and one base pair insertion in the catalytic domain. Previous report showed that all mutant POMGnT1s uniformly lost their enzyme activities [20]. These results imply that additional factor(s) other than enzyme activity of POMGnT1 may play a role in determining disease severity in both brain and skeletal muscle.

Genetic analysis revealed that no mutation was identified in the four patients in our series, which strongly suggest that there still remain other related genes for glycosylation process of α-DG. Careful observation of clinical and pathological findings should help to clarify the precise pathomechaisms of CMD.

Acknowledgements

The authors thank Dr Toda for the information of the primers, and also thank many physicians who provided the clinical information of the patients. This work was supported by Core Research for Evolutional Science and Technology (CREST) from Japan Science and Technology Corporation, and Grants-in-Aid for Research on Psychiatric and Neurological Diseases and Mental Health from the Ministry of Health, Labor, and Welfare.

References

[1] Hayashi YK, Ogawa M, Tagawa K, et al. Selective deficiency of alpha-dystroglycan in Fukuyama-type congenital muscular dystrophy. Neurology 2001;57:115–21.

[2] Kobayashi K, Nakahori Y, Miyake M, et al. An ancient retrotransposal insertion causes Fukuyama-type congenital muscular dystrophy. Nature 1998;394:388–92.

[3] Yoshida A, Kobayashi K, Manya H, et al. Muscular dystrophy and neuronal migration disorder caused by mutations in a glycosyltransferase, POMGnT1. Dev Cell 2001;1:717–24.

[4] Beltran-Valero de Bernabe D, Currier S, Steinbrecher A. Mutations in the *O*-mannosyltransferase gene POMT1 give rise to the severe neuronal migration disorder Walker-Warburg syndrome. Am J Hum Genet 2002;71:1033–43.

[5] Brockington M, Blake DJ, Prandini P, et al. Mutations in the fukutin-related protein gene (FKRP) cause a form of congenital muscular dystrophy with secondary laminin alpha2 deficiency and abnormal glycosylation of alpha-dystroglycan. Am J Hum Genet 2001;69:1198–209.

[6] Brockington M, Yuva Y, Prandini P, et al. Mutations in the fukutin-related protein gene (FKRP) identify limb girdle muscular dystrophy 2I as a milder allelic variant of congenital muscular dystrophy MDC1C. Hum Mol Genet 2001;10:2851–9.

[7] Driss A, Noguchi S, Amouri R, et al. Fukutin-related protein gene mutated in the original kindred limb-girdle MD 2I. Neurology 2003;60:1341–4.

[8] Longman C, Brockington M, Torelli S, et al. Mutations in the human LARGE gene cause MDC1D, a novel form of congenital muscular dystrophy with severe mental retardation and abnormal glycosylation of alpha-dystroglycan. Hum Mol Genet 2003;12:2853–61.

[9] Michele DE, Barresi R, Kanagawa M, et al. Post-translational disruption of dystroglycan–ligand interactions in congenital muscular dystrophies. Nature 2002;418:417–22.

[10] Martin-Rendon E, Blake DJ. Protein glycosylation in disease: new insights into the congenital muscular dystrophies. Trends Pharmacol Sci 2003;24:178–83.

[11] Osawa M, Sumida S, Suzuki N. Fukuyama type congenital progressive muscular dystrophy. In: Fukuyama Y, Osawa M, Saito K, editors. Congenital muscular dystrophies. Elsevier: Amsterdam; 1997. p. 31–68.

[12] Taniguchi K, Kobayashi K, Saito K, et al. Worldwide distribution and broader clinical spectrum of muscle–eye–brain disease. Hum Mol Genet 2003;12:527–34.

[13] Kim DS, Hayashi YK, Matsumoto H, et al. POMT1 mutation results in defective glycosylation and loss of laminin-binding activity in alpha-DG. Neurology 2004;62:1009–11.

[14] Kondo-Iida E, Kobayashi K, Watanabe M, et al. Novel mutations and genotype–phenotype relationships in 107 families with Fukuyama-type congenital muscular dystrophy (FCMD). Hum Mol Genet 1999;8:2303–9.

[15] Brown SC, Torelli S, Brockington M, et al. Abnormalities in alpha-dystroglycan expression in MDC1C and LGMD2I muscular dystrophies. Am J Pathol 2004;164:727–37.

[16] Louhichi N, Triki C, Quijano-Roy S, et al. New FKRP mutations causing congenital muscular dystrophy associated with mental retardation and central nervous system abnormalities Identification of a founder mutation in Tunisian families. Neurogenetics 2004;5:27–34.

[17] Topaloglu H, Brockington M, Yuva Y, et al. FKRP gene mutations cause congenital muscular dystrophy, mental retardation, and cerebellar cysts. Neurology 2003;60:988–92.

[18] Beltran-Valero de Bernabe D, Voit T, Longman C. Mutations in the FKRP gene can cause muscle–eye–brain disease and Walker-Warburg syndrome. J Med Genet 2004;41:e61.

[19] Santavuori P, Somer H, Sainio K, et al. Muscle–eye–brain disease (MEB). Brain Dev 1989;11:147–53.

[20] Manya H, Sakai K, Kobayashi K, et al. Loss-of-function of an *N*-acetylglucosaminyltransferase, POMGnT1, in muscle–eye–brain disease. Biochem Biophys Res Commun 2003;306:93–7.

PERGAMON

Neuromuscular Disorders 15 (2005) 361–363

www.elsevier.com/locate/nmd

Allelic heterogeneity of GNE gene mutation in two Tunisian families with autosomal recessive inclusion body myopathy

R. Amouri[a,*], A. Driss[a,b], K. Murayama[b], M. Kefi[a], I Nishino[b], F. Hentati[a]

[a]*Department of Molecular Neurobiology and Neuropathology, National Institute of Neurology, 1007 La Rabta, Tunis, Tunisia*
[b]*Department of Neuromuscular Research, National Institute of Neuroscience, National Center of Neurology and Psychiatry (NCNP), 4-1-1 Ogawahigashi-cho, Kodaira, Tokyo 187-8502, Japan*

Received 27 July 2004; received in revised form 20 December 2004; accepted 11 January 2005

Abstract

Autosomal recessive hereditary inclusion body myopathy (AR-*HIBM*), with sparing of the quadriceps, is characterized by adult-onset, with weakness and atrophy of distal lower limb muscles, and typical histopathological findings in muscle biopsy. AR hIBM is associated with mutations in the UDP-N-acetylglucosamine 2-epimerase/N-acetylmannosamine kinase (GNE) gene on chromosome 9p12-13 [1]. We report two unrelated Tunisian families with clinical and pathological features of AR HIBM. One distinct homozygous GNE missense mutation, M712T, previously reported in Middle Eastern Jewish patients, and a newly identified one, L379H, were found in one patient from each family. We conclude that AR *HIBM* in Tunisia shows an allelic genetic heterogeneity.

Keywords: AR *HIBM*; Myopathy; Missense mutation

1. Introduction

Hereditary inclusion body myopathy is a unique group of neuromuscular disorders characterized by adult-onset slowly progressive distal and proximal weakness, and a typical muscle pathology including rimmed vacuoles and filamentous inclusions. HIBM could be inherited as autosomal dominant or autosomal recessive trait. The most common form of ethnic-related autosomal recessive HIBM was first described in Iranian Jews as 'vacuolar myopathy sparing the quadriceps' [2]. *Autosomal* recessive *HIBM* is associated with mutations in the UDP-N-acetylglucosamine 2-epimerase/N-acetylmannosamine kinase (GNE; MIM# 603824) gene on chromosome 9p12-13 [1]. The most common mutation was the M712T homozygous missense mutation found in all Middle Eastern families of both Jewish and non-Jewish descent. Because all patients share a common recombinant haplotype a genetic common founder effect has been proposed [1]. In this study, we report clinical data, muscle biopsy findings, and mutation analysis in patients from two unrelated Tunisian families. One family has been previously reported [3].

2. Results

Nine patients belonging to two unrelated families were selected on the presence of autosomal recessive inheritance, muscle biopsy showing rimmed vacuoles in several fibres and genetic linkage to *AR-HIBM* locus on chromosome 9p12-13. A clinical description of family 2 (five patients) have been previously reported by our group [3]. All patients showed a progressive adult-onset myopathy (mean age at onset: 27 years) with symmetrical proximal and distal weakness predominant in the lower limbs with a relative sparing of the quadriceps. Peroneal and pelvic girdle muscles seemed to be firstly involved resulting in steppage and a waddling gait (Table 1). The shoulder girdle became involved later and facial muscles remained unaffected. In the upper limbs, muscle involvement were less severe and involved the shoulder and less severely humeral and hand muscles. Weakness in the legs included mainly the anterior compartment muscles and the proximal muscles except the quadriceps which was mildly involved. The clinical course

* Corresponding author. Tel.: +216 71 564 421; fax: +216 71 565 167.
E-mail address: rim.sam@gnet.tn (R. Amouri).

0960-8966/$ - see front matter © 2005 Elsevier B.V. All rights reserved.
doi:10.1016/j.nmd.2005.01.012

Table 1
Clinical data

	Patient	Age	Age at onset	Gait	CK values	Muscle strength upper limbs			Muscle strengh lower limbs		
						Shoulder girdle	Humeral muscles	Hand muscles	Pelvic girdle	Quadriceps	Peroneal
Family 1	M1	53	26	Bedridden	49.8	1	3	4	0	3	2
	A2	48	30	Bedridden	89	1	3	4	0	3	2
	H3	40	26	Waddling/steppage	840	2	3	5	2	4	3
	K4	29	26	Waddling/steppage	1542	3	4	5	3	4	3

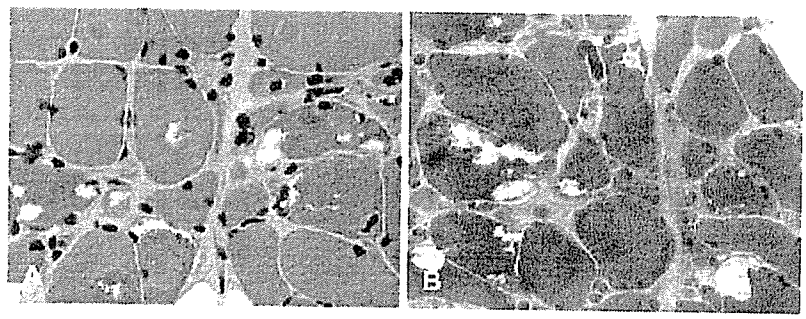

Fig. 1. Muscle biopsy pathology in patient M2 from family 1. HE (A) and Gomori stain (B) demonstrating numerous rimmed vacuoles with fiber changes and central nuclei.

of the disease was variable between siblings. CK levels were moderately elevated (Table 1). EMG showed mixed pattern of 'myogenic and neurogenic' changes as well as myogenic changes similar changes have been found in patients of family 2. Motor and sensory nerve conduction velocities were normal. Normal cerebral MRI was normal in all patients. Asymptomatic periventricular leucoencepahlopathy suspected in patients of family 2 by cerebral CT scan was ruled out by cerebral MRI findings [3].

Rimmed vacuoles were observed in all muscle biopsies of patients from family 2 and only in two out of five in family 1 (Fig. 1). No inflammatory infiltrates were found except for two patients of family 2 where a perivascular inflammation was reported [3].

Peripheral blood samples were obtained with informed consent from 18 family members including the nine patients for DNA analysis. Standard PCR was performed using primers designed to amplify the 13 exons of GNE gene. Sequencing reaction was carried out using an ABI Prism Big-Dye Terminator Cycle. Sequencing kit (Applied Biosystems). The sequence comparison was performed using Sequencher Version 3.11 Software. DNA sample from 100 normal alleles were screened to confirm the mutation.

One patient from each genetically linked family was analyzed for a mutation search. Comparison of both patient's sequences and sequence of a normal control individual revealed the presence of two distinct missense mutations, a T→A transition at position 1187 of exon 7 in family 2 and a T→C transition at position 2186 of exon 12 in family 1 (Fig. 2). The 2186T>C mutation results in

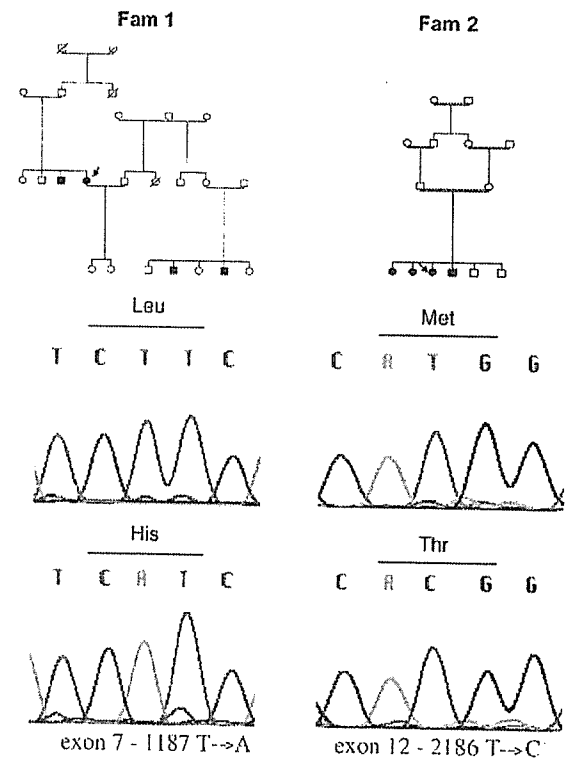

Fig. 2. Electropherograms profiles of mutations. Sequence chromatograms from the control (above) and the mutated (below) individuals. The genotype of both patients shows mutations in GNE gene. Left: shows a T→A transition in exon 7 for family 1 converting leucine to histidine at codon 379 of the peptide sequence. Right: shows a T→C transition in exon 12 for family 2 converting methionine to threonine at the condon 712 of the peptide sequence.

a methionin 712 to threonin amino acid change whereas the 1187T > A predicts to cause a L379H substitution of the peptide sequence.

3. Discussion

In this study, we report two GNE homozygous missense mutations, M712T and L379H, in patients originating from Tunisia with typical clinical and histological features of AR *HIBM*. Rimmed vacuoles were found in deltoid muscle biopsy in two out of five patients in one family, indicating that patients with clinical features of inclusion body myopathy but lacking histological confirmation may nonetheless have GNE inclusion body myopathy. Such findings have been already reported and related to variable muscle involvement [2].

The mutation M712T originally identified in Iranian Jews has been found in all Middle Eastern families of both Jewish and non-Jewish descent and recently in an Italian family [4]. In the Tunisian family carrying this mutation (family 2), the clinical features were similar to those reported in Middle Eastern Jews with symmetrical proximal and distal muscle weakness with relative sparing quadriceps. Interestingly, this homozygous mutation has also been found in two unrelated Muslim families and one from Bedouin origin [5]. A common ancestral mutation shared by Middle Eastern hIBM patients [6] and the Tunisian family cannot be ruled out. Founder effect with unique mutation have been already reported in some neuromuscular disorders in Tunisia such as LGMD 2C [7].

The second mutation reported here, L379H appeared to be a novel one. L379H is located on the amino acid position right next to the D378Y mutation previously reported [5]. This mutation occurred in the epimerase *domain* of the GNE gene in a Tunisian family with particular pathological features such as the inflammatory perivascular infiltrates in muscle biopsy and reported as inclusion body myosistis [3]. A case of *HIBM* combined with muscle inflammation has been recently reported supporting that muscle inflammation is not sufficient to exclude the diagnosis of *HIBM* [8]. The presence of a second mutation in this rare disorder is not in favor of a founder effect and could be explained by de novo mutations revealed by the high rate of consanguineous marriages in Tunisia.

References

[1] Eisenberg I, Avidan N, Potikha T, et al. The UDP-N-acetylglucosamine 2-epimerase/nacetylmannosamine kinase gene is mutated in recessive hereditary inclusion body myopathy. Nat Genet 2001;29:83–7.

[2] Argov A, Yarom R. Rimmed vacuole myopathy sparing the quadriceps: a unique disorder in Iranian Jews. J Neurol Sci 1984;64: 33–43.

[3] Hentati F, Ben Hamida C, Belal S, Tome F, Fardeau M, Ben hamida M. In: Askanas V, Serratrice G, Engel K, editors. Inclusion body myositis and myopathies. Cambridge: Cambridge university press; 1997. p. 211–20.

[4] Broccolini A, Ricci E, Cassandrini D, et al. Novel GNE mutations in Italian families with autosomal recessive hereditary inclusion-body myopathy. Hum Mutat 2004;23(6):632.

[5] Eisenberg I, Grabov-Nardini G, Hochner H, et al. Mutations spectrum of GNE in hereditary inclusion body myopathy sparing the quadriceps. Hum Mutat 2003;21(1):99.

[6] Argov Z, Eisenberg I, Grabov-Nardini G, et al. Hereditary inclusion body myopathy: the Middle Eastern genetic cluster. Neurology 2003; 60(9):1519–23.

[7] Kefi M, Amouri R, Driss A, et al. Phenotypic and sarcoglycans expression in Tunisian LGMD 2C patients sharing the same del521-T mutation. Neuromuscul Disord 2003;13(10):779–87.

[8] Krause S, Schlotter-Weigel B, Walter M, et al. A novel homozygous mutation in GNE gene of a patient with quadriceps sparing hereditary inclusion body myopathy associated with muscle inflammation. Neuromuscul Disord 2003;13:830–4.

J Neuropathol Exp Neurol

Vol. 64, No. 6
June 2005
pp. 513–522

ORIGINAL ARTICLE

Autophagic Vacuoles with Sarcolemmal Features Delineate Danon Disease and Related Myopathies

Kazuma Sugie, MD, PhD, Satoru Noguchi, PhD, Yoshimichi Kozuka, PhD, Eri Arikawa-Hirasawa, MD, PhD, Mikihito Tanaka, PhD, Chuanzhu Yan, MD, Paul Saftig, PhD, Kurt von Figura, PhD, Michio Hirano, MD, Satoshi Ueno, MD, PhD, Ikuya Nonaka, MD, PhD, and Ichizo Nishino, MD, PhD

Abstract

Among the autophagic vacuolar myopathies (AVMs), a subgroup is characterized pathologically by unusual autophagic vacuoles with sarcolemmal features (AVSF) and includes Danon disease and X-linked myopathy with excessive autophagy. The diagnostic importance and detailed morphologic features of AVSF in different AVMs have not been well established, and the mechanism of AVSF formation is not known. To address these issues, we have performed detailed histologic studies of myopathies with AVSF and other AVMs. In Danon disease and related AVMs, at the light microscopic level, autophagic vacuoles appeared to be accumulations of lysosomes, which, by electron microscopy consisted of clusters of autophagic vacuoles, indicative of autolysosomes. Some autolysosomes were surrounded by membranes with sarcolemmal proteins, acetylcholinesterase activity, and basal lamina. In Danon disease, the number of fibers with AVSF increased linearly with age while the number with autolysosomal accumulations decreased slightly, suggesting that AVSF are produced secondarily in response to autolysosomes. Most of the AVSF form enclosed spaces, indicating that the vacuolar membranes may be formed in situ rather than through sarcolemmal indentation. This unique intracytoplasmic membrane structure was not found in other AVMs. In conclusion, AVSF with acetylcholinesterase activity are autolysosomes surrounded by secondarily generated intracytoplasmic sarcolemma-like structure and delineates a subgroup of AVMs.

Key Words: Autophagic vacuole, Autophagy, Danon disease, LAMP-2, Lysosome.

From the Departments of Neuromuscular Research (KS, SN, MT, CY, I Nishino) and Ultrastructural Research (YK), National Institute of Neuroscience, National Hospital for Mental (I Nonaka, I Nishino), Nervous and Muscular Disorders, National Center of Neurology and Psychiatry, Kodaira, Tokyo, Japan; the Department of Neurology (KS, SU), Nara Medical University, Kashihara, Nara, Japan; the Department of Neurology (EA-H), Juntendo University School of Medicine, Tokyo, Japan; the Department of Biochemistry (PS), University of Kiel, Kiel, Germany; Zentrum Biochemie und Moleculare Zellbiologie (PS, KvF), Abteilung Biochemie II, Universität Göttingen, Göttingen, Germany; and the Department of Neurology (MH), Columbia University, New York, New York.

Send correspondence and reprint requests to: Ichizo Nishino, MD, PhD, Department of Neuromuscular Research, National Institute of Neuroscience, National Center of Neurology and Psychiatry (NCNP), 4-1-1 Ogawahigashi-cho, Kodaira, Tokyo 187-8502, Japan; E-mail: nishino@ncnp.go.jp

INTRODUCTION

Danon disease, an X-linked vacuolar cardiomyopathy and myopathy, is caused by primary deficiency of lysosome-associated membrane protein-2 (LAMP-2), a major lysosomal membrane protein (1–4). Muscle biopsies contain small autophagic vacuoles with cytoplasmic debris. The membranes of these vacuoles have structural features of sarcolemma and biochemical activities of acetylcholinesterase (AChE) and nonspecific esterase (NSE) (5). Although some sarcolemmal proteins, including dystrophin, have been detected in vacuolar membranes (3), the presence of other sarcolemmal proteins has not been studied. In addition, the pathomechanism by which LAMP-2 deficiency leads to the formation of these peculiar autophagic vacuoles with sarcolemmal features (AVSFs) is still unknown.

AVSFs are also seen in X-linked myopathy with excessive autophagy (XMEA) (6), infantile autophagic vacuolar myopathy (AVM) (7), and adult-onset AVM with multiorgan involvement (8). XMEA is clinically characterized by a mild pure skeletal myopathy. In contrast, infantile AVM involves both cardiac and skeletal muscles and patients die within several months after birth, whereas adult-onset AVM affects multiple organs including liver, kidney, and skeletal muscles. All of these diseases show multilayered basal lamina and the deposition of C5b-9 over the surface of the muscle fiber; these features are not seen in Danon disease. Nevertheless, these diseases are likely to share a common pathomechanism since they also have AVSF similar to those seen in Danon disease (9).

To delineate subtypes of AVMs and to gain insights into their pathomechanisms, we have performed detailed histologic evaluations of muscle from patients with Danon disease, XMEA, infantile AVM, and adult-onset AVM, and from LAMP-2 deficient mice (10, 11). Moreover, to evaluate the specificity of the AVSF we have also characterized autophagic vacuoles in other lysosomal myopathies, including acid maltase deficiency (AMD), sporadic inclusion body myositis (SIBM), and distal myopathy with rimmed vacuoles (DMRV), which has recently been shown to be the same disease as hereditary inclusion body myopathy (HIBM).

MATERIALS AND METHODS

Patients

We examined skeletal muscles of ten affected men from 8 families with genetically confirmed Danon disease. We also

confirmed this diagnosis by immunohistochemistry to demonstrate absence of LAMP-2 in skeletal muscle. Age at muscle biopsy varied from one year to 29 years, average 15 years ± 9. One patient underwent 2 biopsies from his left biceps brachii muscle at ages one year and from his right quadriceps femoris muscle at age 16 years (12). We also studied muscle from a 2-month-old boy with infantile AVM (7), a 41-year-old man with adult-onset AVM with multiorgan involvement (8), and an 18-year-old man with probable XMEA who showed typical clinicopathologic features of the disease but without a family history of myopathy.

Control specimens were obtained from 10 individuals with morphologically normal muscle. In addition, we also studied muscle from 21 patients with AMD (9 infants, 6 children, and 6 adults), 18 patients with DMRV/HIBM, and 20 patients with SIBM. We confirmed that all DMRV/HIBM patients had mutations in the gene encoding UDP-N-acetylglucosamine 2-epimerase/N-acetylmannosamine kinase (13).

Histochemistry

All biopsy specimens were taken from either the biceps brachii or quadriceps femoris muscle. These tissue samples were frozen in liquid nitrogen-cooled isopentane for histochemistry and immunohistochemistry. Transverse serial frozen sections of 8-μm thickness were stained with hematoxylin and eosin (H&E), modified Gomori trichrome, and a battery of histochemical methods, including AChE and NSE stains.

Immunohistochemistry

We performed indirect immunofluorescence staining on 5-μm serial cryosections of muscle according to previously described methods (14). These sections were incubated at 37°C for 2 hours with primary mouse monoclonal IgG antibodies against AChE, lysosomal membranous proteins: LAMP-1, lysosomal integral membrane protein-1 (LIMP-1), LIMP-2, and 19 primary monoclonal or polyclonal antibodies against various sarcolemmal proteins and extracellular matrix proteins (Tables 1 and 2). We also used antibodies against an intralysosomal protein, cathepsin L, and endosomal proteins, VAMP-7, Rab5, transferrin receptor (TfR), and low-density lipoprotein receptor (LDL-R). These were subsequently incubated at room temperature for 1 hour with a secondary antibody, fluorescein isothiocyanate (FITC)-labeled goat F(ab')2 anti-mouse IgG (Leinco Technology, St. Louis, MO) or anti-rabbit IgG (H&L) (Leinco). For double immunolabeling using mouse monoclonal anti-LIMP-1 and rabbit polyclonal anti-dystrophin antibodies (a generous gift from Dr. Imamura), we used two secondary antibodies: FITC-labeled anti-mouse IgG (Leinco) and rhodamine-labeled anti-rabbit IgG (Leinco). We also have stained serial sections with Alexa 488 conjugated α-bungarotoxin (Molecular Probe, Eugene, OR) and were examined by fluorescence microscopy. Furthermore, in other sections, after incubation with primary antibodies we stained with the avidin-biotin-peroxidase complex method (Vector Laboratories, Burlingame, CA) using another secondary antibody: biotinylated goat anti-mouse IgG (Vector). The reaction was visualized with 3,3'-diaminobenzidine (DAB) as the substrate, yielding a brown reaction product. Normal mouse IgG, diluted to the same concentration as the primary antibodies, was used as a negative control.

To estimate presence of the sarcolemmal proteins in vacuolar membrane, we scored the signal of the antibodies from negative (−) to strong (+++) relative to their immunoreactivity in the sarcolemma. The strong score (+++) indicates that the reactivity level in vacuoles equals that in the sarcolemma. Moreover, we counted the numbers of 1) muscle fibers with intracytoplasmic vacuoles highlighted with dystrophin, and 2) muscle fibers with intracytoplasmic overexpression of LIMP-1, in randomly selected fields of all the patients, and calculated the average percentages of both types of muscle fibers in each patient. Statistical analysis of the correlation between the age of the patients and the numbers of muscle fibers immunoreacting dystrophin or LIMP-1 was performed using linear regression.

Electron Microscopy

For electron microscopy, biopsy specimens were fixed in buffered 2% isotonic glutaraldehyde at pH 7.4, postfixed in osmium tetroxide, and embedded in Epoxy resin. Ultrathin sections were stained with uranyl acetate and lead nitrate, and examined with an H-7000 electron microscope (Hitachi, Tokyo, Japan).

Immunoelectron Microscopy

We performed immunoelectron microscopy by preembedding labeling methods. We used muscle biopsy specimens frozen in liquid nitrogen-cooled isopentane without paraformaldehyde prefixation. The specimens were cut in a cryostat into 10-μm transverse sections without thawing and fixed in chilled 4% paraformaldehyde solution in 0.1M phosphate buffer (pH 7.4) for 10 minutes. The fixed sections were washed 5 times in phosphate-buffered saline (PBS). To eliminate nonspecific reactions, sections were incubated for 30 minutes at room temperature in PBS containing 10% normal goat serum and 1% bovine serum albumin (BSA) with PBS. The sections were then incubated at 4°C overnight with one of the following primary mouse monoclonal IgG antibodies: LIMP-1 and the C-terminus of dystrophin. After washing for 30 minutes in PBS, the sections were incubated at 4°C overnight with a secondary antibody: 10-nm-gold-labeled rat anti-mouse antibody (British Biocell International, Cardiff, UK). Subsequently, the sections were fixed in 0.5% glutaraldehyde and postfixed in osmium, and embedded in Epoxy resin. Ultrathin sections were counterstained with uranyl acetate and lead nitrate.

LAMP-2-Deficient Mice and Pathological Methods

We analyzed tibialis anterior muscle from 2 LAMP-2-deficient mice (10, 11) at ages 4 months and 16 months and age-matched normal mice. Muscle specimens were frozen in liquid nitrogen-cooled isopentane for histochemistry and immunohistochemistry or fixed with glutaraldehyde for electron microscopy. Transverse serial frozen sections of 10-μm thickness were stained with H&E, modified Gomori trichrome,

TABLE 1. Summary of Histochemistry and Immunohistochemistry in Various Myopathies with Autophagic Vacuoles

			Expression on Vacuolar Membrane		
	Manufacturer of Antibody	Dilution	Danon Disease and Related AVMs	Rimmed Vacuolar Myopathies	AMD
Histochemistry					
NSE	–	–	+++	–	–
AChE	–	–	+++	–	–
PAS	–	–	+	–	+++
Acid P	–	–	± to ++	++	++
Immunohistochemistry					
AChE	Chemicon, Temecula, CA	1:2000	+++	–	–
AChR	Molecular Probe, Eugene, OR	1:300	–	–	–
C-terminus of Dystrophin	Novocastra, Newcastle Upon Tyne, UK	1:100	+++	– to +	– to +
Rod domain of Dystrophin	Novocastra	1:50	+++	– to +	– to +
N-terminus of Dystrophin	Novocastra	1:20	+++	– to +	– to +
α-Sarcoglycan	Novocastra	1:100	+++	– to +	– to +
β-Sarcoglycan	Novocastra	1:100	+++	– to +	– to +
γ-Sarcoglycan	Novocastra	1:200	++	– to +	– to +
δ-Sarcoglycan	Novocastra	1:50	+++	– to +	– to +
α-Dystroglycan	Upstate, Lake Placid, NY	1:100	++	– to +	– to +
β-Dystroglycan	Novocastra	1:200	+++	– to +	– to +
Dystrobrevin	RDI, Flanders, NJ	1:100	++	– to +	– to +
Dysferlin	Novocastra	1:50	++	– to +	– to ±
Utrophin	Novocastra	1:50	+	– to ±	–
Caveolin-3	Transduction Labs, Lexington, KY	1:100	++	– to +	– to +
β-Spectrin	Novocastra	1:100	++	– to +	– to +
Laminin α2	Chemicon,	1:5000	++	– to +	– to +
Integrin β1	Genex, Helsinki, Finland	1:100	+++	– to +	– to +
Perlecan	Chemicon	1:100	++	– to +	– to +
Agrin	A generous gift from Dr. Sugiyama (32)	1:100	++	– to +	– to +
Fibronectin	Biomedical Tech., Stoughton, MA	1:1000	++	– to ±	– to ±
Collagen IV	Novocastra	1:1000	– to +	– to ±	– to ±
Collagen VI	ICN, Aurora, OH	1:500	– to +	–	– to ±

Both antibodies against fibronectin and agrin were rabbit polyclonal antibodies. All the other antibodies were mouse monoclonal antibodies. AChR was evaluated by binding to α-bungarotoxin. AMD, acid maltase deficiency; NSE, non-specific esterase; AChE, acetylcholinesterase; PAS, periodic acid Schiff; Acid P, acid phosphatase; AchR, acetylcholine receptor.

and a battery of histochemical methods, and the same immunohistochemical methods described above.

RESULTS

Histochemistry and Immunohistochemistry

By routine histologic studies, the vacuolar membranes in Danon disease, probable XMEA, infantile AVM and adult-onset AVM were essentially identical (Table 1). All muscle samples showed mild to moderate variation in fiber size. There were no necrotic fibers except in muscle from adult-onset AVM, which revealed a few necrotic and regenerating fibers. There were scattered small basophilic granules rather than vacuoles in the muscle fibers in H&E-stained sections (Fig. 1). Histochemistry revealed AChE and NSE activities in the vacuolar membranes and the vacuolar structures of the granules. Immunohistochemistry also confirmed presence of AChE in those vacuoles. However, they did not bind to α-bungarotoxin, indicating the absence of acetylcholine receptors (AChRs) in the vacuolar membranes.

By immunohistochemistry, the AVSF reacted for all the tested sarcolemmal and extracellular matrix proteins in the vacuolar membranes in muscle from patients with Danon disease and related AVMs, although reactivity levels of the proteins were variable (Table 1; Fig. 1). However, only collagens IV and VI showed less intense reactivity in the vacuolar membranes than that in the sarcolemma. Most of the AVSFs were scattered throughout the cytoplasm rather than clustered in the subsarcolemmal region. On serial transverse 5-μm sections, most of the AVSFs formed a closed space and the vacuolar membranes were not connected to the sarcolemma with only a few exceptions (Fig. 1Y). Longitudinal sections demonstrated the oval shape of the AVSF, confirming the closed structure of the vacuoles (Fig. 1Z). Vacuolar membranes connected to the sarcolemma were seen in only 2 patients; both were more than 20 years old.

In muscle from patients with Danon disease, LIMP-1, a lysosomal membrane protein, showed accumulations scattered

TABLE 2. Summary of Lysosomal and Endosomal Proteins for Immunohistochemistry in Danon Disease and Related AVMs

Antigen	Manufacturer	Dilution	Expression in the Muscle Fibers
Lysosomal protein			
LAMP-1	Developmental Studies Hybridoma Bank (DSHB), Iowa City, IA	1:100	++
LAMP-2	DSHB	1:100	–
LIMP-1	DSHB	1:100	+++
LIMP-2	A generous gift from Dr. Tanaka (10)	1:200	+
Cathepsin L	Abcam, Cambridge, UK	1:100	+
Endosomal protein			
Rab5	BD Bioscience, Franklin Lakes, NJ	1:50	+
LDL-R	Progen Biotechnik, Heidelberg, Germany	1:100	+
VAMP-7	A generous gift from Dr. Galli (29)	1:200	++
Transferrin R	Lab Vision, Fremont, CA	1:100	+

Antibody against LIMP-2 was rabbit polyclonal and antibody against LDL-R was chicken polyclonal. All the other antibodies were mouse monoclonal.

throughout the fibers in a distribution identical to that of the small basophilic granules on H&E-stained sections (Fig. 2; Table 2), indicating that most autophagic vacuoles in Danon disease are autolysosomes. These autolysosomal accumulations were surrounded by dystrophin-positive membranes in some fibers but not in others (Fig. 2). LAMP-1 and LIMP-2 showed slightly increased expression in fibers with LIMP-1-positive granules (data not shown). Muscle fibers with dystrophin-positive vacuoles accounted for 0.5% to 14.3%, increasing in proportion with age ($y = 0.016 + 0.40x$, $r = 0.94$; Fig. 3). Muscle fibers with autolysosomal accumulations, both with and without dystrophin-positive vacuolar membranes, accounted for 23.7% to 28.7%, showing a slight tendency to decrease with age ($y = 28.6 - 0.15x$, $r = 0.71$; Fig. 3).

LDL-R, TfR, and Rab5 showed mild upregulation mainly in fibers with autolysosomal accumulations in Danon disease and related AVMs (Table 2). Cathepsin L was expressed weakly, mainly in fibers with autolysosomal accumulations. Only VAMP-7 was strongly expressed, mainly in the non-vacuolated fibers without autolysosomal accumulations.

There were occasional intracytoplasmic vacuoles with sarcolemmal proteins in muscles from patients with other AVMs (i.e. DMRV/HIBM, SIBM, and AMD) but their presence was less consistent than in Danon disease and related AVMs. In addition, they never showed AChE or NSE activity. In DMRV/HIBM and SIBM, fibers with sarcolemmal protein-associated vacuoles accounted for approximately 5% to 15% of fibers with rimmed vacuoles (Fig. 4; Table 1). In AMD, sarcolemmal and extracellular matrix proteins were present in some vacuolar membranes. The frequency of fibers with sarcolemmal proteins-associated vacuoles was less than 5% of vacuolated fibers in infantile AMD, and 10% to 15% of vacuolated fibers in childhood and adult-onset AMD.

Electron Microscopy and Immunoelectron Microscopy

In Danon disease and related AVMs, electron microscopy revealed scattered clusters of autophagic vacuoles containing cytoplasmic debris, electron dense materials, and myeloid bodies. Some of these autophagic vacuoles had basal lamina on the luminal side, while other clusters were not limited by a membrane (Fig. 5).

Immunoelectron microscopy showed many autophagic vacuoles; however technical limitations posed by preparing samples from frozen tissue without prefixation prevented us from clearly defining vacuolar membranes. At higher magnification, dystrophin signals were detected on the cytoplasmic side of the vacuolar membrane and along the periphery of the vacuoles (Fig. 5). In contrast, the LIMP-1 antibody signals were associated with autophagic materials including glycogen particles and cytoplasmic debris within the vacuoles, suggesting that the vacuoles are limited by membranes with sarcolemmal features and contain multiple small autophagic vacuoles derived from autolysosomes.

Muscle Pathology in Mice

Muscles from LAMP-2-deficient mice at both 4 and 18 months of age showed features of AVSFs at both light and electron microscopic levels. There were slight variations in fiber size and small vacuoles with basophilic granules by H&E. The granules contained acid phosphatase-positive material. These AVSFs had AChE and NSE activities similarly to those in Danon disease. The frequency of muscle fibers with the AVSFs decorated by NSE and AChE activities was 0.4% at 4 months and 8% at 16 months (data not shown). On immunohistochemistry, the vacuolar membranes were stained with antibodies against dystrophin and other sarcolemmal proteins as well as extracellular matrix proteins, whereas LAMP-2 was completely absent in the muscle. On electron microscopy, there were scattered intracytoplasmic autophagic vacuoles with glycogen particles and cytoplasmic debris (data not shown).

DISCUSSION

In muscle from patients with Danon disease and related AVMs, the membranes of AVSF showed immunoreactivity for all of the sarcolemmal and extracellular matrix proteins tested. Dystrophin and dystrobrevin are cytoskeletal proteins localized along the cytoplasmic side of the sarcolemma (15). Sarcoglycans and β-dystroglycan are transmembranous proteins and are components of "dystrophin bolts" (16). Utrophin

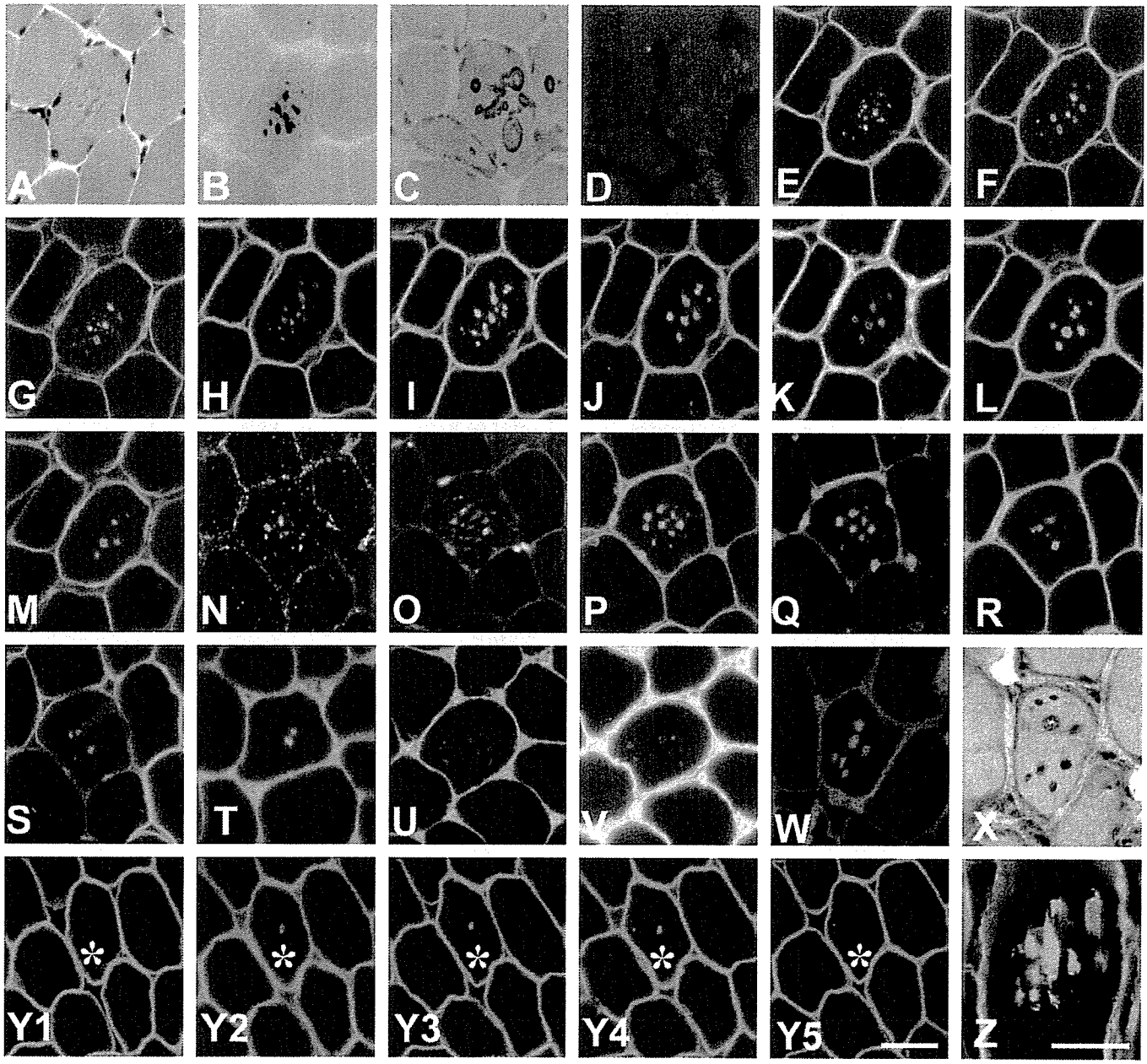

FIGURE 1. Histochemistry and immunohistochemistry. Transverse sections of skeletal muscle biopsies from Danon disease patients. Several fibers contain scattered tiny basophilic intracytoplasmic vacuoles (**A**): H&E. The vacuolar membrane has high nonspecific esterase (**B**) and acetylcholinesterase (**C**) activities. None of the vacuoles bind to α-bungarotoxin (**D**). Sections were stained with antibody against the C-terminus of dystrophin (**E**), the rod domain of dystrophin (**F**), the N-terminus of dystrophin (**G**), laminin α2 (**H**), α-sarcoglycan (**I**), β-sarcoglycan (**J**), γ-sarcoglycan (**K**), δ-sarcoglycan (**L**), dystrobrevin (**M**), α-dystroglycan (**N**), utrophin (**O**), dysferlin (**P**), β-dystroglycan (**Q**), perlecan (**R**), caveolin-3 (**S**), collagen IV (**T**), fibronectin (**U**), collagen VI (**V**), integrin β1 (**W**), and agrin (**X**). The vacuolar membranes were immuno-positive with most of the primary antibodies, although reactivity of these proteins was variable. The results are summarized in Table 1. Transverse 5-μm serial sections (**Y1–Y5**) and longitudinal section (**Z**) of muscle from Danon disease patient showing immunoreaction for dystrophin. Vacuolar membrane in muscle fiber (*) is not connected to the sarcolemma but is closed. Longitudinal section shows that the vacuoles are spherical or oval. (**D–W, Y1–Y5, Z**): FITC-labeled staining; (**X**): DAB staining. (**C–S, U, V, Y1–Y5**): serial sections. Scale bars: (**A–W, Y1–Y5**) = 20 μm; (**Z**) = 30 μm.

is a submembranous protein structurally similar to dystrophin and is widely expressed, albeit at low levels, in the sarcolemma (17). Integrin β1 and α7 are transmembranous proteins and form a complex with each other in the sarcolemma (18). Dysferlin and caveolin-3 are also sarcolemmal proteins and are responsible for limb-girdle muscular dystrophy (LGMD) 2B and LGMD 1C, respectively (19, 20). Extracellular proteins, collagen IV, perlecan, fibronectin, agrin, and laminin, are the

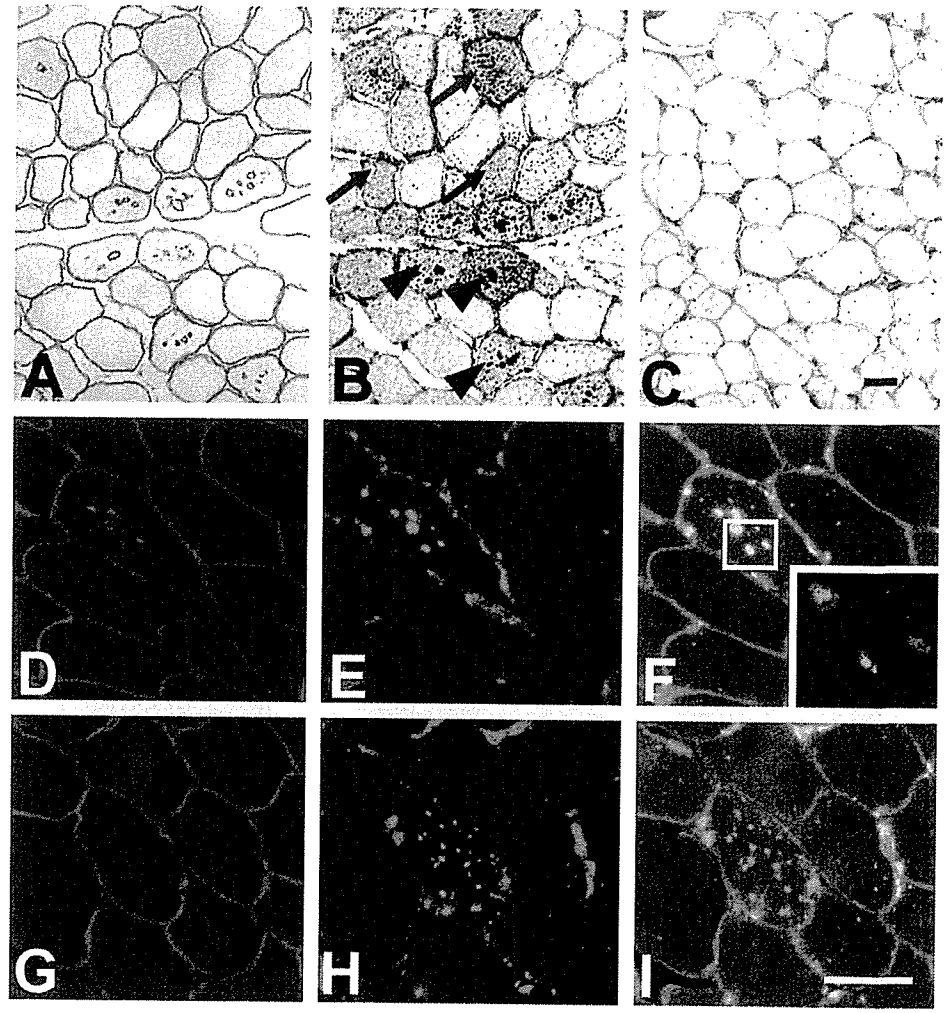

FIGURE 2. Indirect immunohistochemistry. Transverse sections of skeletal muscle stained with DAB for dystrophin **(A)** and LIMP-1 **(B, C)**. **(A, B)** Danon disease patient; **(C)**: Normal control. In Danon disease some muscle fibers express both LIMP-1 and dystrophin (arrowheads), whereas some muscle fibers show overexpression of LIMP-1 with absence of dystrophin (arrows). Normal control showed almost no expression of LIMP-1 **(C)** in muscle fibers. Scale bar = 40 μm. Double immunohistochemistry. Transverse sections of skeletal muscle from Danon disease patient, stained for dystrophin and LIMP-1. LIMP-1 is strongly accumulated inside the muscle fibers **(D, G)**. In some muscle fibers, LIMP-1-positive accumulations are clearly surrounded by dystrophin immunopositive membrane **(D–F)**. These vacuoles are the AVSF. In other muscle fibers, LIMP-1-positive accumulations are not surrounded by dystrophin **(G–I)**. **(D, G)**: dystrophin; **(E, H)**: LIMP-1; **(F, I)**: merged. Scale bar = 30 μm.

main components of the basal lamina. Collagen VI is present in the interstitium but is associated directly with collagen IV (21). We observed very little staining of only collagens IV and VI in vacuolar membranes, indicating that the membranes hardly contain these collagens. Based on our findings, we deduce that the vacuolar membrane of AVSFs in Danon disease and related AVMs have most of the sarcolemmal proteins ranging from cytoplasmic dystrophin to the extracellular laminin.

The vacuolar membranes of AVSF have abundant activities of AChE similar to neuromuscular junctions. Nevertheless, they are distinct from motor endplates because the membranes lacked AChRs. In the early stages of formation of the neuromuscular junction, AChE and AChRs are localized diffusely throughout the sarcolemma. When axon terminals make contact with muscle cells, postjunctional folds are quickly formed. In this process, AChE and AChRs accumulate at junctions and disappear from the extra-junctional sarcolemma (22, 23). These facts support our hypothesis that the vacuoles are intracellular enclosed spaces, because, if AVSF were derived from sarcolemma, then AChE-expressing vacuoles should be located near neuromuscular junctions rather than scattered in the cytoplasm. Furthermore, the presence of AChE without AChRs clearly indicates that the vacuolar membranes are distinct from either junctional or extra-junctional sarcolemma and suggests that they are formed through a unique process.

In the intracellular degradative process called autophagy, "isolation membranes" initially sequesters portions of cytoplasm to be degraded and forms "autophagosomes," which then fuse with lysosomes and become "autolysosomes." The cytoplasm sequestered in autolysosomes is then digested by proteolytic enzymes provided by the lysosomes. Most autophagic vacuoles in Danon disease are autolysosomes rather than autophagosomes, which lack enzymatic activity. These are indicated by the demonstration of many LIMP-1-positive accumulations scattered throughout the fibers (24, 25) and the autophagic nature of the vacuoles on electron microscopy. Actually, small basophilic granules on hematoxylin and eosin are most likely these autolysosomal accumulations as suggested by their pattern of distribution and the fact that lysosomes are basophilic on H&E. Moreover, some clusters of autolysosomes are surrounded by membranes with sarcolemmal features but others are not. In support of this notion, ultrastructural studies identified 2 types of autophagic vacuoles: 1) clusters of autophagic vacuoles not surrounded by membranes or basal lamina, and 2) vacuoles containing various